Letter

Capillary Sorting of Particles by Dip Coating

B.M. Dincau,[1] M.Z. Bazant,[2,3] E. Dressaire,[1] and A. Sauret[1,*]

[1] *Department of Mechanical Engineering, University of California, Santa Barbara, California 93106, USA*
[2] *Department of Chemical Engineering, Massachusetts Institute of Technology, Cambridge, Massachusetts 02139, USA*
[3] *Department of Mathematics, Massachusetts Institute of Technology, Cambridge, Massachusetts 02139, USA*

(Received 19 March 2019; revised manuscript received 10 May 2019; published 16 July 2019)

In this letter, we describe the capillary sorting of particles by size based on dip coating. A substrate withdrawn from a liquid bath entrains a coating whose thickness depends on the withdrawal speed and the liquid properties. If the coating material contains particles, they will only be entrained when the viscous force pulling them with the substrate overcomes the opposing capillary force at the deformable meniscus. This force threshold occurs at different liquid thicknesses for particles of different sizes. Here, we show that this difference can be used to separate small particles from a mixed suspension through capillary filtration. In a bidisperse suspension, we observe three distinct filtration regimes. At low capillary numbers, Ca, no particles are entrained in the liquid coating. At high Ca, all particle sizes are entrained. For a range of capillary numbers between these two extremes, only the smallest particles are entrained while the larger ones remain in the reservoir. We explain how this technique can be applied to polydisperse suspension. We also provide an estimate of the range of capillary number to separate particles of given sizes. The combination of this technique with the scalability and robustness of dip coating makes it a promising candidate for high-throughput separation or purification of industrial and biomedical suspensions.

DOI: 10.1103/PhysRevApplied.12.011001

Suspensions of particles are common throughout industrial, geophysical, and biomedical materials [1–3]. These disciplines all share a demand for scalable size-based particle separation techniques [4,5], which can be utilized for high-volume sample analysis, preparation of highly uniform suspensions, or purification [6]. Different techniques that use particle, flow, and geometry interactions have been developed to achieve separation [7,8]. A conventional method is direct filtration through a semipermeable filter or membrane [9]. This has the disadvantage of periodic filter replacement [10]. Numerous inertial microfluidic techniques have emerged, which can separate particles based on size without relying on replaceable filters but still suffer from a relatively low per-unit throughput, with maximum reported values on the order of milliliters per minute [11–13]. This, combined with their susceptibility to clogging [14–20], has made scalability a significant challenge for microfluidic separation techniques. Different methods that use external fields to further influence particle motion have also been developed [21–24]. Despite their potential for improved efficiency, these techniques are more complicated to scale up and their reliance on external fields necessitates that they are system specific, limiting the variety of the suspensions that they can process.

Recent work in filtration has resulted in the development of soft filtration techniques, which use a liquid interface as a tunable filter. This approach has been demonstrated using the liquid film produced by a moving bubble [25] and with freestanding liquid surfaces [26], but neither of these techniques possesses the scalability required for large-scale applications. Froth floatation is a three-phase separation process based on the manipulation of the difference in hydrophobicity of suspended solids. While highly scalable, this technique cannot differentiate particles based on size [27].

In this work, we introduce a technique for size-based particle separation using a dip-coating system. We show that the competition between viscous forces and surface tension at the meniscus can serve as a tunable dynamic filter, giving rise to a clog-free separation technique with promising scalability.

Dip coating is a process through which the withdrawal of a substrate from a liquid reservoir is used to deposit a uniform liquid coating [28–30]. The thickness of the coating, h, depends on the withdrawal speed U, the fluid viscosity η, and the surface tension γ. These three parameters are combined in the capillary number $\mathrm{Ca} = \eta U/\gamma$, which describes the ratio of viscous to capillary forces. The coating thickness is given by $h = 0.94\,\ell_c\,\mathrm{Ca}^{2/3}$ according to the Landau-Levich-Derjaguin (LLD) prediction for

*asauret@ucsb.edu

small Ca, where $\ell_c = \sqrt{\gamma/(\rho g)}$ is the capillary length [28,29]. When dip coating is used for a continuous-sheet substrate, the coating process can run indefinitely so long as the reservoir is replenished [31,32]. This combination of scalability and robustness has made dip coating a popular technique, which is appealing for filtration applications [31].

Recent results have shown that particle entrainment in dip coating of suspensions only occurs above a threshold velocity [33–36]. This is due to a competition of forces at the meniscus, which forms where the substrate meets the liquid-air interface. The viscous force during withdrawal acts to pull particles with the substrate, while the capillary force opposes the deformation of the meniscus and prevents large particles from entering the coating film. Both of these forces depend on the particle size but at different rates, resulting in a unique entrainment threshold for each size. In this letter, we demonstrate that this force balance can be leveraged to design a capillary filter, in which careful selection of the capillary number results in the filtration of smaller particles, while leaving larger particles in the reservoir. We experimentally investigate this filtration approach and demonstrate its feasibility in separating particles from a bidisperse suspension.

To study how capillary filtration can be used to separate particles based on size, we work with the experimental setup illustrated in Fig. 1, which consists of a glass plate mounted in a fixed position above a suspension of silicone oil (AP100, Sigma Aldrich, density $\rho = 1058\ \mathrm{kg\,m^{-3}}$, dynamic viscosity $\eta = 0.132$ Pa s, surface tension $\gamma = 21\ \mathrm{mN\,m^{-1}}$ at 20 °C) and polystyrene microparticles (Dynoseeds, density $\rho_P \simeq 1055\ \mathrm{kg\,m^{-3}}$), with diameters $2a = [88, 140, 240]\ \mu$m. Silicone oil provides complete wettability of the particles and substrate; however, it has been demonstrated that substrate wettability has little effect on the particle-entrainment threshold [37]. The particles

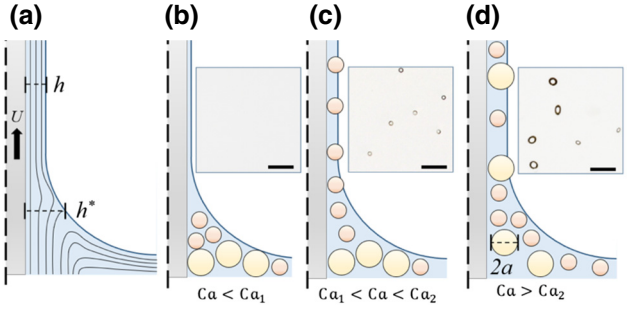

FIG. 1. (a) Qualitative fluid streamlines, with the withdrawal speed U, film thickness h, and stagnation thickness h^*. (b)–(d) Three coating regimes for a bidisperse suspension. (b) At low Ca, no particles are entrained. (c) At intermediate Ca, only the small particles are entrained. (d) At high Ca, both small and large particles are entrained. The insets show examples of entrained films in each regime. The scale bars are 500 μm.

are neutrally buoyant over the time scale of an experiment. The reservoir is mounted on a movable stage controlled by a linear motor (ThorLabs NRT150). The volume fraction of the suspensions $\phi = V_p/V_T$, defined as the volume of particles V_p divided by the total volume $V_T = V_p + V_f$, is maintained at $\phi \leq 1\%$. Each trial involves a substrate withdrawal at a velocity $0.05\ \mathrm{mm\,s^{-1}} < U < 1\ \mathrm{mm\,s^{-1}}$. A camera (Nikon D7200) with a 200-mm macrolens is used to photograph the plate after withdrawal.

During withdrawal, the plate is coated with a liquid layer of thickness $h = 0.94\,\ell_c\,\mathrm{Ca}^{2/3}$. The thickness at the stagnation point h^* in the meniscus is given by $h^*/\ell_c = 3\,(h^*/\ell_c) - (h^*/\ell_c)^3/\mathrm{Ca}$ and limits the size of particles that can enter the film [33,36]. In a sense, the meniscus acts as a deformable filter, which excludes particles that are too large to pass. Therefore, tuning Ca controls the size threshold for particle entrainment. With our setup, we vary Ca by controlling the withdrawal speed U, which in turn influences the stagnation thickness h^* and determines the maximum particle size entrained. With increasing Ca, we note qualitatively three distinct coating regimes for a bidisperse suspension. At low Ca, no particles are entrained [Fig. 1(b)]. For high Ca, both particle sizes are entrained [Fig. 1(d)]. For Ca values between these two, only the smaller particles are entrained [Fig. 1(c)] and we note this to be the capillary-filtration regime. In the following, we use our experimental setup to characterize the filtration regime, by studying, first, monodisperse suspensions and then bidisperse suspensions.

We begin with a series of experiments on monodisperse suspensions to estimate the range of the filtration regime and the number of particles that are filtered. In Fig. 2, we report the results of experiments performed with a monodisperse suspension ($2a = 240\,\mu$m, $\phi_{240} = 0.625\%$). After each trial, we count the number of particles per unit area N_A on the plate. We also introduce N_V, the number of particles per unit volume in the bulk suspension, which is equal to the prepared volume fraction ϕ multiplied by the volume of a single spherical particle such that $N_v = 4/3\,\pi\,a^3\,\phi$. When the particles are expected to be entrained, i.e., when the thickness of the coating film is large enough, N_A and N_V are related through the thickness of the fluid coating h: $N_A = N_V\,h$. We plot a theoretical value of N_A/N_V based on the LLD prediction for h when the particles are not filtered (NF):

$$\left.\frac{N_A}{N_V}\right|_{\mathrm{NF}} = 0.94\,\ell_c\,\mathrm{Ca}^{2/3}. \tag{1}$$

In Fig. 2, we show the evolution of N_A with the capillary number. We observe that Eq. (1) agrees well with the experimental results in the yellow region. Here, the viscous force that entrains the particle in the liquid film is larger than the capillary force that would keep the particle in the liquid bath corresponding to a soft filter larger

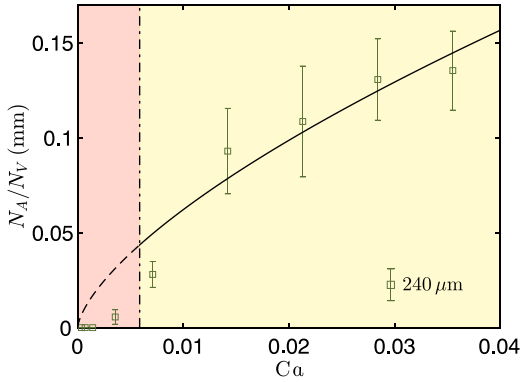

FIG. 2. Data from a series of monodisperse filtration trials with $2a = 240$ μm particles. Experimental measurements are shown in green. The dashed and the continuous lines indicate h as governed by the LLD law, in the region where the theory is not expected and expected to apply, respectively. At sufficiently large Ca (yellow region), particle entrainment follows the theoretical prediction based on the volume of fluid entrained [Eq. (1)]. Below the entrainment threshold (red region), particles are excluded by capillary forces at the meniscus, resulting in a large disparity between theoretical and measured entrainment. A vertical dash-dotted line for this threshold is shown at $\mathrm{Ca}^* = 0.24\, Bo^{3/4} \simeq 6 \times 10^{-3}$.

than the particle size. The particle is entrained passively with the liquid and the volume fraction in the coating film is similar to the volume fraction ϕ in the bulk suspension. For low enough Ca, this relationship breaks down as particles are trapped at the meniscus and do not coat the substrate, as observed in the red region: the soft filter is smaller than the particle size. The transition between the two regimes at Ca^* determines when capillary filtration is possible: when $\mathrm{Ca} < \mathrm{Ca}^*$, particles can be filtered out of the liquid film, whereas when $\mathrm{Ca} > \mathrm{Ca}^*$, particles are entrained in the liquid film.

The capillary threshold for particle entrainment, Ca^*, depends on the particle size through the Bond number of the particle $\mathrm{Bo} = (a/\ell_c)^2$, $\mathrm{Ca}^* = 0.24\, Bo^{3/4}$ [33,36]. Recently, this relationship has been experimentally demonstrated across different particle sizes and working fluids [35,37]. Note that this transition does not correspond to an inertial effect, as $Re \ll 1$ for all of the experimental data. In Fig. 2, the predicted threshold value is $\mathrm{Ca}^* = 6 \times 10^{-3}$ [36], which is in good agreement with our measurements. In the following, we take advantage of this relationship by tuning Ca to filter suspensions.

To demonstrate this, we perform experiments for two bidisperse suspensions of different size ratios a_B/a_S, where a_B and a_S are the radii of the big and small particles in the suspensions, respectively. Here, we consider (i) $2\,a_S = 88$ μm and $2\,a_B = 240$ μm and (ii) $2\,a_S = 88$ μm and $2\,a_B = 140$ μm. We consider a low volume fraction, $\phi_B + \phi_S = 1\%$ to avoid cluster formation and limit the change of viscosity. In addition, the volume-fraction ratio ϕ_B/ϕ_S is such that the number of small particles is not too large compared to the number of large particles [25]. The results are reported in Figs. 3(a) and 3(b). Since h is determined only by the fluid properties and the withdrawal speed, N_A/N_V can be used to normalize the results above the threshold capillary number Ca^*, as demonstrated first in Fig. 2. This allows us to directly compare the entrainment of particles having different sizes and volume fractions. The evolution of N_A/N_V should remain the same across different particle suspensions, as predicted in Eq. (1). For the bidisperse suspensions, we observe a clear range in which capillary filtration occurs. In Fig. 3(a), we note a capillary-filtration regime of approximately $5 \times 10^{-4} < \mathrm{Ca} < 3.5 \times 10^{-3}$ for separating 88-μm particles from 240-μm particles. In this range, the number of 88-μm particles entrained scales with the volume of fluid entrained, dictated by h, because $\mathrm{Ca} > \mathrm{Ca}^*_{88}$. On the other hand, 240-μm particle entrainment falls significantly short in this region, because $\mathrm{Ca} < \mathrm{Ca}^*_{240}$. We note that this region has a range of $\Delta\mathrm{Ca} = 3 \times 10^{-3}$. The optimal capillary number to achieve filtration is thus at a value

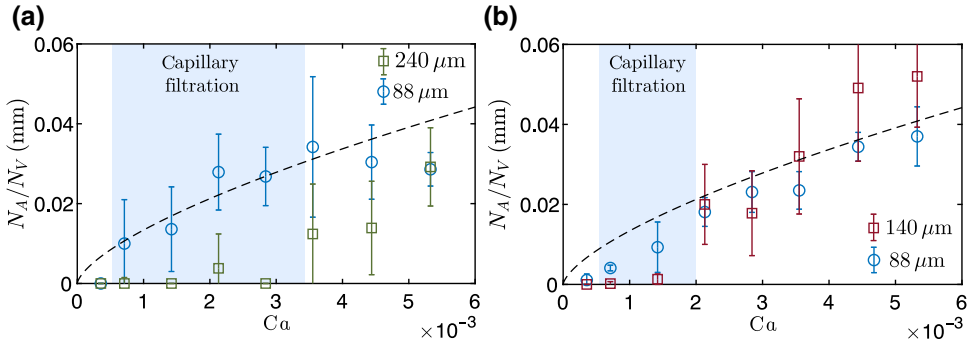

FIG. 3. Data from two filtration experiments with bidisperse suspensions: (a) 88 μm (blue circles) and 240 μm (green squares) at $\phi_{88} = 0.09\%$ and $\phi_{240} = 0.91\%$; (b) 88 μm (blue circles) and 140 μm (red squares) at $\phi_{88} = 0.17\%$ and $\phi_{140} = 0.83\%$. The filtration regime is highlighted in blue, where 88-μm particles are separated from larger particles in the suspension. At low Ca, very few or no particles are entrained; while at high Ca, both particle sizes are entrained at similar relative quantities.

slightly smaller than Ca^*_{240}, where the number of small particles entrained will be the largest and equal to $N_A \simeq 0.94\,\ell_c\,{Ca^*_{240}}^{2/3}\,N_{V,88}$, in which $N_{V,88} = 4/3\,\pi\,{a_{88}}^3\,\phi_{88}$, so that $N_A \simeq 3.94\,\ell_c\,{Ca^*_{240}}^{2/3}\,{a_{88}}^3\,\phi_{88}$. In Fig. 3(b), we see that the effective range of capillary filtration is significantly reduced when separating 88-μm particles from 140-μm particles, at approximately $5 \times 10^{-4} < Ca < 2 \times 10^{-3}$. In this case, $\Delta Ca = 1.5 \times 10^{-3}$.

The range of capillary number can limit the filtration resolution when the particles are too close in size. To estimate ΔCa, we consider that a particle of radius a_S will be entrained for $Ca > Ca^*_S = 0.24\,{Bo_S}^{3/4}$. Similarly, a second larger particle of radius a_B will remain in the liquid bath for $Ca < {Ca_B}^* = 0.24\,{Bo_B}^{3/4}$. Therefore, the capillary-filtration range is

$$\Delta Ca = Ca^*_B - Ca^*_S = 0.24\left(\frac{a_B}{\ell_c}\right)^{3/2}\left[1 - \left(\frac{a_S}{a_B}\right)^{3/2}\right]. \tag{2}$$

Using this expression, we find that the predicted capillary-filtration range for the 240-μm/88-μm bidisperse suspension is $\Delta Ca_{240/88} = 3.3 \times 10^{-3}$ and for the 140-μm/88-μm suspension $\Delta Ca_{140/88} = 1.3 \times 10^{-3}$. These values are in good agreement with the values measured experimentally. Capillary filtration via dip coating may be best suited for applications in which ΔCa is large, corresponding to the situation in which the filtered particles are significantly smaller than others, which may often be the case in removing large defects from industrial coatings or for biosample purification (e.g., bacteria of approximately 1 μm from mammalian cells of approximately 10 μm). It has been demonstrated that bioparticles follow an entrainment scaling similar to that of inert particles [36].

The efficiency of the filtration process within the range of capillary number allowing separation is illustrated in Fig. 4. The histograms represent the size distribution of the particles in the suspension (before the capillary filtration) on the top half and on the plate (after capillary filtration) on the bottom half. The large particles are completely removed while all the small particles are entrained, which results in a very similar probability distribution. If one were to filter a polydisperse suspension, successive dip-coating experiments with varying capillary numbers would allow the removal of particles of unwanted size while retaining particles of desired sizes.

Besides, the upper and lower filtration limits allow estimation of the maximum theoretical throughput for capillary filtration via dip coating. Given particles of radius a, substrate width W, withdrawal speed U, coating thickness h, and fluid properties η, ρ, and γ, the maximum withdrawal speed that does not entrain large particles, reached at Ca^*_B, is for $U^*_B \simeq 0.24(\gamma/\eta)(a_B/\ell_c)^{3/2}$. Thus

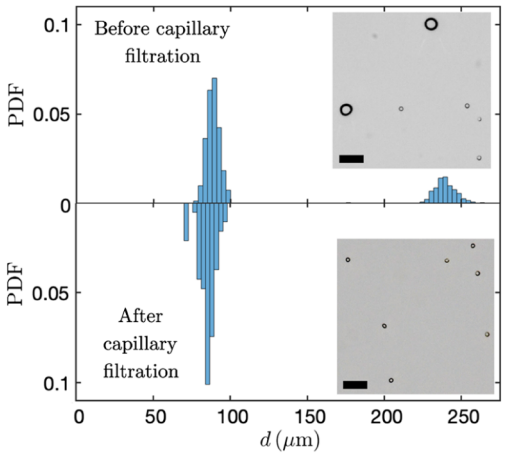

FIG. 4. An example of capillary sorting of a bidisperse suspension: 88 μm and 240 μm at 0.91% and 0.09%, respectively. The experiment is performed at $Ca = 3 \times 10^{-3}$ and demonstrates that the particles collected in the liquid film are only the smallest ones. The insets show bidisperse suspension before (top) and after (bottom) the capillary filtration. Scale bars are 500 μm.

the maximum particle throughput for a continuous planar substrate is given by $Q_p = 0.24\,w\,h\,(\gamma/\eta)(a/\ell_c)^{3/2}\,\phi$. Separated particles could be collected either by physical exclusion using a wiper or by withdrawing the coated substrate from a secondary reservoir at a lower Ca [38].

A challenge with this method is that at higher volume fraction ϕ, particles can assemble into clusters in the meniscus and be entrained at a threshold capillary number Ca^* smaller than the expected value, thus reducing the range of ΔCa over which capillary filtration is possible [36]. In addition, as large particles are filtered at the meniscus, the local volume fraction ϕ increases. This increases the local viscosity η [39,40] and the local Ca. This aspect is best mitigated by working with dilute suspensions, which has the disadvantage of lowering effective particle throughput. However, of all the soft filtration techniques recently proposed [25,26], capillary filtration via dip coating possesses the greatest scalability to overcome the necessity for dilute suspensions.

Finally, we note that we apply this separation technique using a single working fluid and hence a single set of fluid properties. However, this technique relies only on the entrainment threshold for individual particles, which has been characterized by previous work across a broad range of particle sizes and working fluids [35,37]. Therefore, nondimensionalization by the capillary and Bond numbers will allow future application of this technique.

In this letter, we demonstrate the selective exclusion of large particles at the meniscus of a dip-coating interface in a capillary-filtration process. When suspended particles differ in size, smaller particles can be selectively removed at the appropriate Ca, while larger particles remain in the

bath. We experimentally show that this technique can separate particles in a bidisperse suspension. We quantify the separation range to give some insight into the resolution of this technique and provide an estimate for maximum theoretical throughput for any dip-coating filtration system using a planar substrate. The combination of this mechanism with the scalability and robustness of dip coating represents a promising approach for high-throughput size-based filtration.

ACKNOWLEDGMENTS

We are grateful to H. A. Stone and G. M. Homsy for helpful discussions.

[1] J. D. Schwarzkopf, M. Sommerfeld, C. T. Crowe, and Y. Tsuji, *Multiphase Flows with Droplets and Particles* (CRC Press, Boca Raton, FL, 2011).
[2] J. J. Stickel and R. L. Powell, Fluid mechanics and rheology of dense suspensions, Annu. Rev. Fluid Mech. **37**, 129 (2005).
[3] E. Guazzelli and J. F. Morris, *A Physical Introduction to Suspension Dynamics* (Cambridge University Press, Cambridge, UK, 2011).
[4] W. R. Bowen and F. Jenner, Theoretical descriptions of membrane filtration of colloids and fine particles: an assessment and review, Adv. Colloid Interface Sci. **56**, 141 (1995).
[5] L. Svarovsky, *Solid-Liquid Separation* (Elsevier, London, UK, 2000).
[6] S. M. Badenes, T. G. Fernandes, C. A. Rodrigues, M. M. Diogo, and J. M. Cabral, Microcarrier-based platforms for in vitro expansion and differentiation of human pluripotent stem cells in bioreactor culture systems, J. Biotechnol. **234**, 71 (2016).
[7] A. Lenshof and T. Laurell, Continuous separation of cells and particles in microfluidic systems, Chem. Soc. Rev. **39**, 1203 (2010).
[8] B. M. Dincau, Y. Lee, J.-H. Kim, and W.-H. Yeo, Recent advances in nanoparticle concentration and their application in viral detection using integrated sensors, Sensors **17**, 2316 (2017).
[9] R. W. Baker, *Membrane Technology and Applications* (John Wiley & Sons, Hoboken, NJ, 2012).
[10] D. Urfer, P. M. Huck, S. D. J. Booth, and B. M. Coffey, Biological filtration for bom and particle removal: a critical review, J. Am. Water Works Assoc. **89**, 83 (1997).
[11] D. Mark, S. Haeberle, G. Roth, F. von Stetten, and R. Zengerle, Microfluidic lab-on-a-chip platforms: requirements, characteristics and applications, Chem. Soc. Rev. **39**, 1153 (2010).
[12] D. T. Chiu, A. J. de Mello, D. D. Carlo, P. S. Doyle, C. Hansen, R. M. Maceiczyk, and R. C. Wootton, Small but perfectly formed? successes, challenges, and opportunities for microfluidics in the chemical and biological sciences, Chem **2**, 201 (2017).
[13] J. Zhang, S. Yan, D. Yuan, G. Alici, N.-T. Nguyen, M. E. Warkiani, and W. Li, Fundamentals and applications of inertial microfluidics: a review, Lab Chip **16**, 10 (2016).
[14] H. M. Wyss, D. L. Blair, J. F. Morris, H. A. Stone, and D. A. Weitz, Mechanism for clogging of microchannels, Phys. Rev. E **74**, 061402 (2006).
[15] C. Henry, J.-P. Minier, and G. Lefèvre, Towards a description of particulate fouling: From single particle deposition to clogging, Adv. Colloid Interface Sci. **185**, 34 (2012).
[16] G. C. Agbangla, É Climent, and P. Bacchin, Experimental investigation of pore clogging by microparticles: evidence for a critical flux density of particle yielding arches and deposits, Sep. Purif. Technol. **101**, 42 (2012).
[17] A. Sauret, E. C. Barney, A. Perro, E. Villermaux, H. A. Stone, and E. Dressaire, Clogging by sieving in microchannels: application to the detection of contaminants in colloidal suspensions, Appl. Phys. Lett. **105**, 074101 (2014).
[18] G. C. Agbangla, P. Bacchin, and E. Climent, Collective dynamics of flowing colloids during pore clogging, Soft Matter **10**, 6303 (2014).
[19] E. Dressaire and A. Sauret, Clogging of microfluidic systems, Soft Matter **13**, 37 (2017).
[20] A. Sauret, K. Somszor, E. Villermaux, and E. Dressaire, Growth of clogs in parallel microchannels, Phys. Rev. Fluids **3**, 104301 (2018).
[21] S. Fiedler, S. G. Shirley, T. Schnelle, and G. Fuhr, Dielectrophoretic sorting of particles and cells in a microsystem, Anal. Chem. **70**, 1909 (1998).
[22] D. Holmes and H. Morgan, in *European Cells and Materials* (2002), Vol. 4, p. 120.
[23] K. Grujic, O. G. Hellesø, J. P. Hole, and J. S. Wilkinson, Sorting of polystyrene microspheres using a y-branched optical waveguide, Opt. Express **13**, 1 (2005).
[24] P. Sajeesh and A. K. Sen, Particle separation and sorting in microfluidic devices: a review, Microfluid. Nanofluid. **17**, 1 (2014).
[25] Y. E. Yu, S. Khodaparast, and H. A. Stone, Separation of particles by size from a suspension using the motion of a confined bubble, Appl. Phys. Lett. **112**, 181604 (2018).
[26] B. B. Stogin, L. Gockowski, H. Feldstein, H. Claure, J. Wang, and T.-S. Wong, Free-standing liquid membranes as unusual particle separators, Sci. Adv. **4**, eaat3276 (2018).
[27] B. Shean and J. Cilliers, A review of froth flotation control, Int. J. Miner. Process. **100**, 57 (2011).
[28] L. Landau and B. Levich, Dragging of a liquid by a moving plate, Acta Phys. URSS **17**, 42 (1942).
[29] B. Derjaguin and A. Titievskaya, Experimental study of liquid film thickness left on a solid wall after receeding meniscus, Dokl. Akad. Nauk USSR **50**, 307 (1945).
[30] E. Rio and F. Boulogne, Withdrawing a solid from a bath: How much liquid is coated?, Adv. Colloid Interface Sci. **247**, 100 (2017).
[31] L. Scriven, Physics and applications of dip coating and spin coating, MRS Online Proc. Library Arch. **121**, 717 (1988).
[32] D. Quéré, Fluid coating on a fiber, Annu. Rev. Fluid Mech. **31**, 347 (1999).

[33] C. E. Colosqui, J. F. Morris, and H. A. Stone, Hydrodynamically driven colloidal assembly in dip coating, Phys. Rev. Lett. **110**, 188302 (2013).

[34] J. C. Kao and A. Hosoi, Spinodal decomposition in particleladen landau-levich flow, Phys. Fluids **24**, 041701 (2012).

[35] A. Gans, E. Dressaire, B. Colnet, G. Saingier, M. Z. Bazant, and A. Sauret, Dip-coating of suspensions, Soft Matter **15**, 252 (2019).

[36] A. Sauret, A. Gans, B. Colnet, G. Saingier, M. Z. Bazant, and E. Dressaire, Capillary filtering of particles during dip coating, Phys. Rev. Fluids **4**, 054303 (2019).

[37] S. Palma and H. Lhuissier, Dip-coating with a particulate suspension, J. Fluid Mech. **869** (2019).

[38] S. Khodaparast, F. Boulogne, C. Poulard, and H. A. Stone, Water-based peeling of thin hydrophobic films, Phys. Rev. Lett. **119**, 154502 (2017).

[39] I. E. Zarraga, D. A. Hill, and D. T. Leighton Jr., The characterization of the total stress of concentrated suspensions of noncolloidal spheres in newtonian fluids, J. Rheol. **44**, 185 (2000).

[40] F. Boyer, É Guazzelli, and O. Pouliquen, Unifying suspension and granular rheology, Phys. Rev. Lett. **107**, 188301 (2011).